

# Rapid experience-dependent plasticity of synapse function and structure in ferret visual cortex in vivo

Hongbo Yu<sup>1,2</sup>, Ania K. Majewska<sup>1,3</sup>, and Mriganka Sur<sup>4</sup>

Department of Brain and Cognitive Sciences, Picower Institute for Learning and Memory, Massachusetts Institute of Technology, Cambridge, MA 02139

Edited\* by Jon H. Kaas, Vanderbilt University, Nashville, TN, and approved November 10, 2011 (received for review May 26, 2011)

**The rules by which visual experience influences neuronal responses and structure in the developing brain are not well understood. To elucidate the relationship between rapid functional changes and dendritic spine remodeling in vivo, we carried out chronic imaging experiments that tracked visual responses and dendritic spines in the ferret visual cortex following brief periods of monocular deprivation. Functional changes, which were largely driven by loss of deprived eye responses, were tightly regulated with structural changes at the level of dendritic spines, and occurred very rapidly (on a timescale of hours). The magnitude of functional changes was correlated with the magnitude of structural changes across the cortex, and both these features reversed when the deprived eye was reopened. A global rule governed how the responses to the two eyes or changes in spines were altered by monocular deprivation: the changes occurred irrespective of regional ocular dominance preference and were independently mediated by each eye, and the loss or gain of responses/spines occurred as a constant proportion of predeprivation drive by the deprived or nondeprived eye, respectively.**

cortical circuits | ocular dominance plasticity | optical imaging | two-photon imaging

Experience-dependent plasticity in the primary visual cortex (i.e., V1) is a proving ground for understanding how the quality and quantity of input activity influences cortical synapses and circuits. In particular, blocking or reducing activity in one eye during a critical period of development leads to a physiological loss of responses to stimulation of the deprived eye and an increase of responses to the nondeprived eye (1, 2). The dynamics of ocular dominance (OD) plasticity are key to understanding its mechanisms. Initial estimates (2) suggested that functional changes in OD preference could occur with 3 to 6 d of monocular deprivation (MD). Subsequent experiments demonstrated that a saturating functional shift of OD preference required several days of MD at the peak of the critical period (3, 4). However, a significant reduction in deprived eye responses can be recorded even after a few hours of deprivation (5). Recent experiments have shown that the reduction of responses from the deprived eye occurs rapidly, followed by a slower increase of drive from the nondeprived eye (6, 7). Recovery of deprived eye responses after eye reopening occurs robustly (8, 9), although its time course has not been well studied.

The structural basis of OD plasticity has also been studied at different timescales, but the mechanisms for rapid loss and recovery of responses remain unresolved. Several weeks of MD in cats leads to a shrinkage of deprived eye thalamocortical arbors and an expansion of nondeprived eye arbors (10, 11). However, 2 d of MD has no effect on the relative numerical synaptic density or synaptic vesicle protein density in deprived and nondeprived afferents (12). In contrast, 7 d of MD causes a decrease in the total length of deprived-eye geniculocortical arbors (10). Changes in intracortical connections can occur rapidly, but still have been described on the order of a few days (13).

One possible locus of rapid physiological and anatomical change is at the level of dendritic spines, which contain the postsynaptic elements of excitatory synapses (14) and are known to be important for compartmentalizing synaptic signals (15). Spines are motile structures (16, 17) whose dynamics are likely to

have a role in their functional properties (18). Spines' size (19, 20) and persistence (20, 21) are influenced by persistent changes in synaptic efficacy. In visual cortex, spine length is decreased and spines are destabilized by prolonged dark-rearing (22, 23), and spine density and motility are altered after several days of MD (24, 25). Thus, brief periods of MD and recovery may also rapidly alter spine structure and distribution. In this study, we combined two-photon microscopy and intrinsic signal imaging in the same region of ferret V1 in vivo, and measured the morphological arrangement of dendritic spines together with the functional shift elicited by short-term MD and recovery from MD. We found rapid, correlated changes in functional visual drive and dendritic morphology after short-term manipulation.

## Results

### Imaging Visual Drive and Dendritic Structure in Visual Cortex in Vivo

**Over Time.** To determine structural and functional changes in cortical neurons in vivo over time, we developed a chronic window preparation that allowed relatively noninvasive repeat imaging of these two properties in V1 (area 17) of young ferrets near the peak of the critical period for OD plasticity [approximately postnatal day 40 (4)]. The local functional mapping of the activity-dependent hemodynamic signal was obtained by intrinsic signal imaging of activity elicited by visual stimulation of each eye independently (Fig. 1*A*). To assay neuronal structure, a mutant Sindbis virus delivering EGFP (26) was focally injected into visual cortex at the time of window preparation to label neurons (Fig. 1*B*), allowing visualization of dendritic spines with the use of two-photon microscopy (Fig. 1*C–F*). These injections labeled many neurons, the majority of which were layer 2/3 cells (Fig. 1*C* and Fig. S1), although a small proportion of the imaged dendritic sections may have come from deeper layer neurons that project to the pial surface. Individual neurons could often be reconstructed in detail, and their processes compared reliably over time (Fig. S1). The images obtained in two-photon and intrinsic signal imaging modalities were aligned based on the blood vessel pattern (Fig. 1*A–C*). The OD index (ODI) could be measured separately for each pixel (Fig. 1*A* and *B*) along with the addition or loss of spines underlying the same pixels (Fig. 1*C–F*; *SI Materials and Methods* includes details of analysis), allowing us to correlate functional changes within small regions of V1 and structural changes of synapses in precisely the same regions.

Author contributions: H.Y., A.K.M., and M.S. designed research; H.Y. and A.K.M. performed research; H.Y. and A.K.M. analyzed data; and H.Y., A.K.M., and M.S. wrote the paper.

The authors declare no conflict of interest.

\*This Direct Submission article had a prearranged editor.

<sup>1</sup>H.Y. and A.K.M. contributed equally to this work.

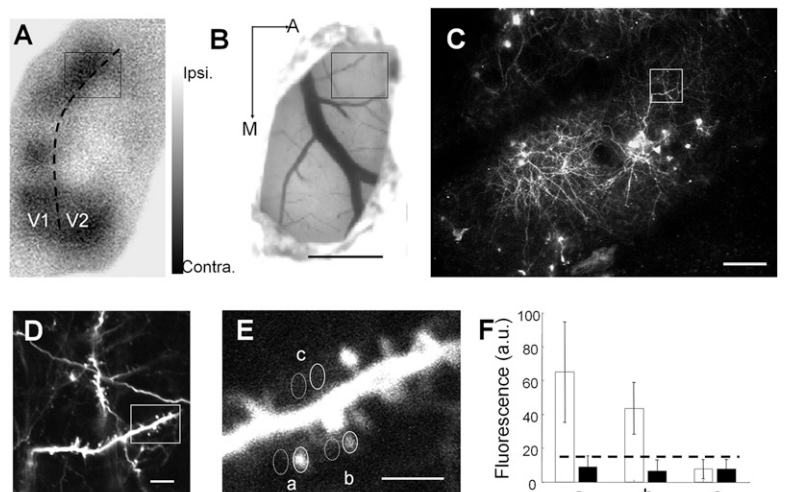
<sup>2</sup>Present address: Center for Brain Science Research and School of Life Sciences, Fudan University, Shanghai 200433, China.

<sup>3</sup>Present address: Department of Neurobiology and Anatomy, Center for Visual Science, University of Rochester, Rochester, NY 14642.

<sup>4</sup>To whom correspondence should be addressed. E-mail: msur@mit.edu.

This article contains supporting information online at [www.pnas.org/lookup/suppl/doi:10.1073/pnas.1108270109/-DCSupplemental](http://www.pnas.org/lookup/suppl/doi:10.1073/pnas.1108270109/-DCSupplemental).

**Fig. 1.** Chronic functional and structural imaging of the ferret primary visual cortex in vivo. (A) OD map of primary visual cortex in a ferret measured by intrinsic signal optical imaging (at 630 nm). Pixels from black to white represent the level of contralateral to ipsilateral eye drive according to key (Right). Dotted line shows the border of V1 (area 17) and V2 (area 18). (B) Blood vessel map (at 546 nm) corresponding to A. EGFP-expressing virus was injected into the boxed area, and a chronic transparent window was implanted above the exposed cortex for repeated optical and two-photon imaging. (C) Magnified image of the boxed area from A and B shows EGFP-labeled cells and their processes imaged by using two-photon microscopy (low digital zoom, magnification of 1×). The region and its processes can be precisely aligned with the functional OD map, based on the blood vessel pattern in B. (D) Magnified image of the boxed area in C shows labeled dendrites and axons. (E) Magnified image of the boxed area in D shows dendritic spines. This image corresponds approximately to a single pixel in A and B, allowing dendritic spine structure to be correlated with functional eye-specific drive on a pixel-by-pixel basis. Individual spines were outlined to measure the fluorescence of all pixels, and only the spines with an average fluorescence 1 SE higher than the neighboring neuropil (stippled circles in E) were counted as existing spines. (F) Quantification of fluorescent intensity (arbitrary units) for the three labeled spines and neighboring neuropil areas in E. Stippled line shows the detection threshold. Notice that area c falls below the detection threshold and was not counted as a spine. (Scale bars: A and B, 1 mm; C, 100 μm; D, 20 μm; E, 5 μm.)



**Rapid and Long-Term Changes in Functional Responses Elicited by MD.** To determine the timescales of functional changes induced by MD, we chronically monitored the functional OD shift at multiple time points of MD in window-implanted ferrets. Fig. 2 shows the intrinsic signal imaged in the same area of V1 in a P42 ferret before MD, at early and late time points after MD, and after eye reopening to show the timescales of recovery of the OD map. Imaging was always carried out in the hemisphere contralateral to the deprived eye. In normal young ferrets, the cortical response was biased toward the contralateral eye (Fig. 2A), as described previously (27, 28). However, even after very short time periods of MD (3 h), the deprived eye response decreased substantially, whereas the nondeprived eye response increased slightly, leading to a significant shift of the OD map toward the nondeprived eye (Fig. 2A–C). This shift was enhanced after prolonged MD (7 d). Reopening the deprived eye led to a rapid (within 3 h) partial recovery of deprived eye responses, with nearly full recovery of the OD map to control levels after 1 d. The rapid OD shifts during MD and recovery periods were consistently observed in a population of ferrets: after 3 to 6 h of MD or recovery, OD was significantly altered (OD before MD,  $-3.3 \pm 0.9 \times 10^{-3}$ ; OD after MD,  $7.0 \pm 0.4 \times 10^{-3}$ ; OD recovery,  $-4.0 \pm 1.2 \times 10^{-3}$ ;  $P < 0.05$  comparing post-MD with pre-MD or recovery;  $n = 4$  ferrets; ANOVA; Fig. 2D).

**Rapid Global Changes in Cortical Drive Elicited by MD.** To understand the spatial dynamics and distribution of this remarkably rapid shift in responses away from the deprived eye following MD, we analyzed changes in drive from the deprived and nondeprived eye to all the pixels within an imaged map. It should be noted that the set of pixels in a map has varying amounts of input from each eye to each pixel, leading to a wide distribution of OD values across the map. We wished to examine whether OD changes were dependent on interactions between the two eyes and hence most profound in binocular regions where the two eyes each provide substantial input, or whether they were instead independent of the degree of drive from each eye and expressed uniformly across the map. A pixel-based analysis revealed that, during short-term MD, the OD map shifted globally: regardless of the extent of binocularity, all cortical pixels shifted their OD preference toward the nondeprived eye (Fig. 3A and B). The correlation between the single pixel ODI before and after MD was almost linear ( $r = 0.99$ ;  $P < 0.05$ ), with a global elevation of the curve toward nondeprived eye dominance even in strongly deprived eye-dominated regions (Fig. 3C).

To further examine these findings, we investigated the deprived and nondeprived eye responses separately. After 6 h of MD, deprived eye responses decreased significantly. However, the fine structure of the OD map was unchanged, with an absolute difference map (i.e., pre-MD – MD) similar to the pre-MD map (Fig. 3D). Specifically, an analysis for each animal revealed a mean global 40% loss of deprived eye responses

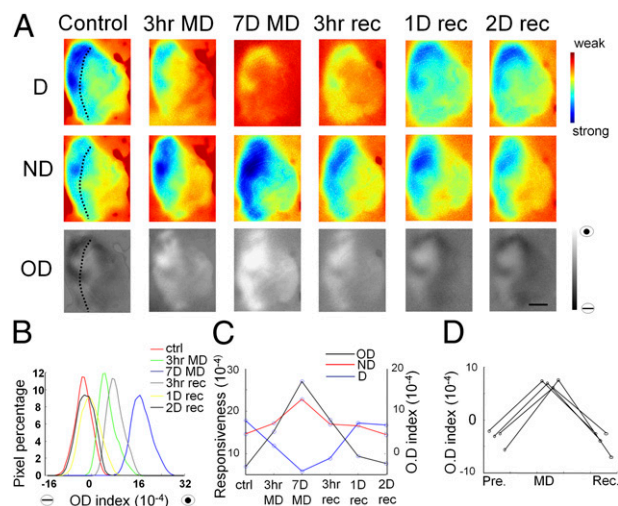


**Fig. 2.** Rapid OD shift evoked by MD and recovery in ferret V1. (A) Changes in deprived eye response (D), nondeprived eye response (ND), and ODI maps, measured by repetitive intrinsic signal optical imaging of the same region of V1 within a span of 9 d. Following the control image, the eyelid of the contralateral eye was sutured first for 3 h, opened briefly for a short-term MD data point (3 h MD), sutured immediately for 7 d, then opened for a long-term MD data point (7D MD), and left open for 2 d to enable successive recovery period data points [3 h, 1 d (1D), and 2 d (2D) recovery]. (Scale bar: 1 mm.) Dotted line shows the border of area 17 and 18. (B) Histograms of the ODI of all of the pixels in the map. Higher values represent nondeprived eye-dominated responses. (C) Mean deprived (blue) and nondeprived (red) eye responsiveness and ODI (black) at different time points. The values of all of the cortical pixels in the map were averaged for each corresponding time point. It is interesting to note that the MD effect is not linear across time: the initial 3 h MD evoked a similar ODI shift as the 3 h to 7 d MD. (D) Rapid OD shifts in four ferrets, evoked by 3 to 6 h MD and immediately followed by 3 to 6 h of recovery from MD.

$[(\text{pre-MD} - \text{MD}) / \text{pre-MD}]$  throughout the cortex, and a slight, nonsignificant 10% increase of nondeprived eye responses, regardless of the OD preference of the imaged region ( $n = 4$ ; Fig. 3E). Thus, MD for even a few hours leads to a rapid global reduction of responses from the deprived eye that is proportional to the pre-MD drive, so that pixels with high pre-MD drive have a greater absolute reduction than pixels with low drive. Plotting the response strengths of each pixel before and after MD for each eye independently yielded linear correlations that paralleled unity for each eye in each animal (Fig. S2). Although the deprived eye showed a uniform decrease in cortical drive for all animals, the response of the nondeprived eye generally showed little change (except in one animal in which nondeprived eye responses were enhanced following short-term MD). The change in deprived and nondeprived eye were not correlated (Fig. S3).

These findings point to rapid functional changes initiated by MD, with a depression of deprived eye responses that depends largely on the level of deprived-eye pre-MD drive. We simulated a global shift in OD on experimental maps obtained from ferrets before MD, and compared them with the map obtained after MD (*SI Materials and Methods*). We applied a global fixed-ratio fluctuation of deprived and nondeprived eye responses independently (i.e., activity-dependent model) and found that simulated maps closely matched experimental maps obtained after short-term MD (Fig. 4; Fig. S4 shows additional examples). In contrast, a competitive model in which the effect of MD depended on binocular interactions (*SI Materials and Methods*) yielded results that differed greatly from experimental data (Fig. 4B, D, and E).

**Imaging Structural Correlates of Rapid OD Plasticity.** These physiological findings suggest specific, and even surprising, predictions for their underlying structural basis, including changes in spine number in specific OD domains following MD (as detailed later).

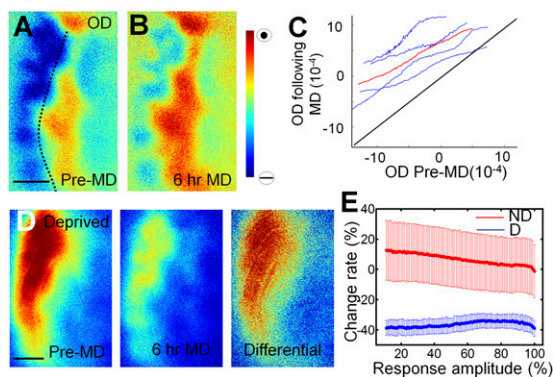


**Fig. 3.** A global shift of OD is evoked by brief MD. (A and B) OD maps of the same visual cortex before (A) and after 6 h of MD (B). Dotted line shows the border of area 17 and 18. (C) Pixel-to-pixel correlation of ODI before and after MD. Blue, four individual ferrets; red, average of four animals. The entire set of pixels was divided into 100 bins according to their ODI percentile before MD; the same group of pixels in each bin was then averaged after MD. Notice the ODI shift toward the nondeprived eye in monocular and binocular regions. (D) Greater loss of absolute responsiveness in deprived eye-dominated regions. The differential map (comparing pre-MD control and after MD) resembles the control map pattern. (E) Graph shows proportional change in responsiveness for the deprived and nondeprived eyes. The x axis shows the degree of pre-MD response from either eye across the pixels of the map; pixels can vary from near 0% to near 100% response amplitude from each eye. The y axis shows the shift in relative response after MD; note that both the deprived ("D") and nondeprived ("ND") lines are nearly horizontal, indicating that the percent response change is independent of the initial responsiveness of pixels to one or the other eye. Thus, although the proportional change is uniform, deprived eye-dominated regions show greater absolute loss of responses. (Scale bars: 1 mm.)

To test these predictions, we examined the structure of dendritic spines and their loss or gain after short-term MD by imaging the same spines before and after MD and correlating their structure with their functional OD domain. First, we established the reliability of repeated dendritic imaging, overall effects of MD and recovery, and features of spines in ferret V1. Within an experimental time window of 1 to 2 d, the GFP labeling of neurons remained stable: dendritic arbor tips were located at the same positions (Fig. S1), the majority of dendritic spines remained stable (rates of spine loss and gain  $<10\%$ ; 10 sites in four ferrets, 962 spine pairs,  $96 \pm 17$  spines and  $2.8 \pm 0.62$  dendrites per site; Fig. 5A and D), and the total spine number did not change (Fig. 5C). However, after a brief period of MD (6 h), spine turnover increased significantly, with a larger percentage of spines being lost rather than gained (Fig. 5B and D). This led to a small but significant decrease in the total spine number ( $10 \pm 2\%$ ; 29 sites from six ferrets, 2,602 spine pairs,  $90 \pm 11$  spines and  $3.24 \pm 0.33$  dendrites per site;  $P < 0.05$ ). When MD was followed by a 24-h period of recovery (i.e., the deprived eye was reopened) dendritic spines were gained and the spine number returned to pre-MD levels ( $P > 0.2$ , comparing control and MD animals after the recovery period; Fig. 5C). Some new spines ( $\sim 40\%$ ) appeared at the same location where a spine had previously been lost during MD, but most spines were made at new dendritic locations (Fig. 5B and Fig. S5). Overall, the rates of spine loss and gain were both higher than in control non-MD animals ( $P < 0.05$ ; Fig. 5D).

To determine whether there were any morphological changes in stable spines elicited by short-term MD and recovery from MD, we characterized spines according to their morphological classifications in two animals (29). Although dendritic spine morphology exists as a continuum, different behaviors have been assigned to spines with different structures (30). Therefore, we classified dendritic spines into mushroom, thin, and stubby types based on their length and spine head volume, as previously described (31), and also quantified the number of filopodia (which were rare at these ages). Throughout the short-term manipulation, we observed

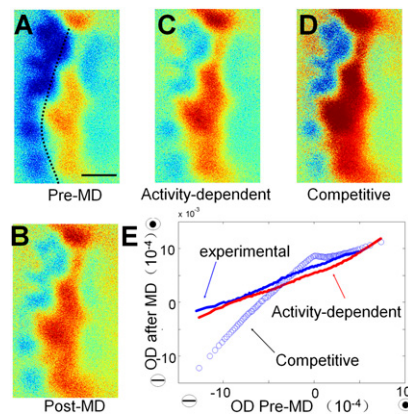


**Fig. 4.** An activity-dependent model simulates experimental OD changes. (A–D) OD maps before MD (A), after MD (B), and simulated after MD by using an activity-dependent model with a global shift (C) and a competitive model (D). Dotted line shows the border of area 17 and 18. Simulation was applied to the deprived and nondeprived eye response maps before MD. In the activity-dependent model, the response amplitudes of all of the pixels in the deprived eye map were reduced by 40%, whereas all pixels in the nondeprived eye map were increased by 10%. The simulated OD map is the differential map between these two shifted maps. In the competitive model, pixels were altered by 25% based on the binocularity index (*SI Materials and Methods*). (E) Close correlation between the experimental and activity-dependent simulated OD maps after MD but not the competitive simulated OD maps. All the pixels of the control OD map were binned into 100 groups according to their percentile ODI, and the means of the same group of pixels were calculated in experimentally shifted OD map after MD and simulated OD maps.

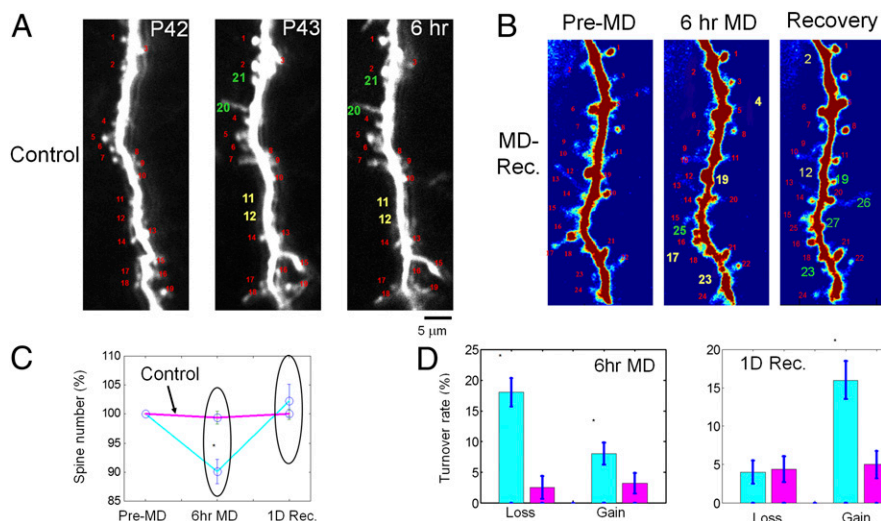


**Fig. 5.** Rapid remodeling of dendritic spines after short-term MD and recovery from MD. Spine turnover in the primary visual cortex of (A) a control ferret and (B) a ferret with MD. Red, intact spines; yellow, lost spines; green, new spines (based on comparison with the initial imaging session). Note that spines 23 and 19 in B reappear after the recovery period, whereas other spines (spines 26 and 27) are made at new locations at this imaging time point. (C) Short-term MD induces a significant decrease in spine number, which reverses after the eye is reopened (blue line). No changes in spine number were observed in control animals (pink line). (D) MD and recovery periods affect the turnover of spines. Spine loss and gain were increased by MD and recovery. Blue bars represent MD and pink bars represent control (\* $P < 0.05$  vs. control).

similar proportions of spine morphological types (Fig. S6), suggesting that there is no large-scale reorganization in dendritic spine morphology on a population level during brief manipulations of experience. Additionally gained and lost spines were unlikely to be mature, mushroom spines (distribution of the 442 lost and 191 gained spines was 21% mushroom, 42% stubby, 25% thin, and 12% filopodia). The rapid reduction of spine number by MD, and its restoration following recovery after MD, is consistent with the rapid functional shift we observed using intrinsic signal imaging, suggesting that there is a close correspondence between functional and structural remodeling.

#### Correlating Structural and Functional Remodeling Following MD.

Based on the physiological findings demonstrating independent changes in the deprived and nondeprived eye after MD, we hypothesized that short-term MD independently influences particular subsets of dendritic spines that mediate input from one eye or the other. Fig. S7 graphically presents changes in spine number as a function of deprived and nondeprived eye drive during visual manipulations in an idealized model. Briefly, regions that are dominated by the deprived eye would see a severe reduction of drive, and show the most effect on spine structure, likely by a major reduction of spines (Fig. S7C). As we saw a slight enhancement in the strength of the nondeprived eye, we also expected that all regions would show some independent effect of response enhancement from the nondeprived eye (in proportion to their pre-MD nondeprived eye drive) as a small gain of spines. Regions receiving input predominantly from the nondeprived eye would show the most gain of spines (Fig. S7D).

To determine whether these predictions hold in vivo, dendritic spines in regions of different OD preference were monitored before and after short-term MD (Fig. 6A). Interestingly, we observed that, in deprived eye regions, many spines were lost following MD compared with nondeprived eye regions, where spines were not lost or were sometimes gained (Fig. 6A). In our population of ferrets (six ferrets, 29 sites), we observed a positive correlation whereby there was greater spine loss, less spine gain, and a decrease in total spine number in deprived eye-dominated regions. This was reversed in nondeprived eye-dominated regions [ $r = 0.58$ ,  $P < 0.05$  (Fig. 6B);  $r = 0.56$ ,  $P < 0.05$  (Fig. 6C);  $r = 0.33$ ,  $P < 0.05$  (Fig. 6D)]. The changes in spine loss and gain as a function of OD are consistent with the predictions of our model (Fig. S7), and demonstrate a close correlation between functional plasticity of eye-specific visual responses and structural plasticity of spines.

#### Discussion

The structural basis of rapid functional changes, and the extent of morphological and functional remodeling of synapses during OD plasticity, is not well understood. Here we used imaging approaches to simultaneously monitor neuronal response properties and synaptic structure in ferret V1 over several days after manipulations of visual experience through unilateral lid suture. We describe rapid functional OD plasticity mediated largely by a profound loss of deprived eye responses, which can be equally rapidly reversed by reopening the deprived eye. Pixel-by-pixel analysis suggests that a global rule governs how the responses to the two eyes are altered by MD across cortex: the changes occur irrespective of regional OD preference and are independently mediated by each eye, and the change in responses occurs as a constant proportion of pre-MD drive by each eye. Interestingly, structural plasticity of dendritic spines closely follows functional plasticity both in time course and underlying rule: local V1 regions experience rapid spine loss in proportion to deprived eye drive.

Such a rule needs to be implemented by specific mechanisms. In the companion paper (32), we use a Förster resonance energy transfer-based probe to demonstrate that CaMKII is a key factor in spine loss and preservation: spines within deprived-eye zones in which CaMKII is activated are preserved, whereas spines with low basal CaMKII are lost.

**Rapid OD Plasticity in V1.** Although, traditionally, OD plasticity was studied by using long-duration MD, it is clear that OD shifts can occur in as little as 1 d or even a few hours in cats. However, it is unclear whether the same mechanisms are responsible for the effects of short- and long-term MD. Understanding such relationships requires examination of the OD map chronically in the same animal through these different manipulations. Early chronic imaging studies showed that long-term MD resulted in a remodeling of the OD map such that nondeprived eye-dominated regions expanded at the expense of deprived eye-dominated regions (11). Because such expansion and shrinkage would occur at the interface between the two eye domains in the binocular zone, this suggested that the greatest plasticity occurred in areas driven by both eyes. Here we show that the mechanisms of short-term MD may be very different from those observed following long-term MD. After 3 to 6 h of MD in the ferret, we found that the OD map shifted linearly in all the regions of cortex, irrespective of OD preference. Changes were not most pronounced in the binocular zone, but instead were most observed in regions dominated by the deprived eye, consistent with the proposal that such rapid effects are driven largely by the rapid loss of deprived eye responses through a mechanism that

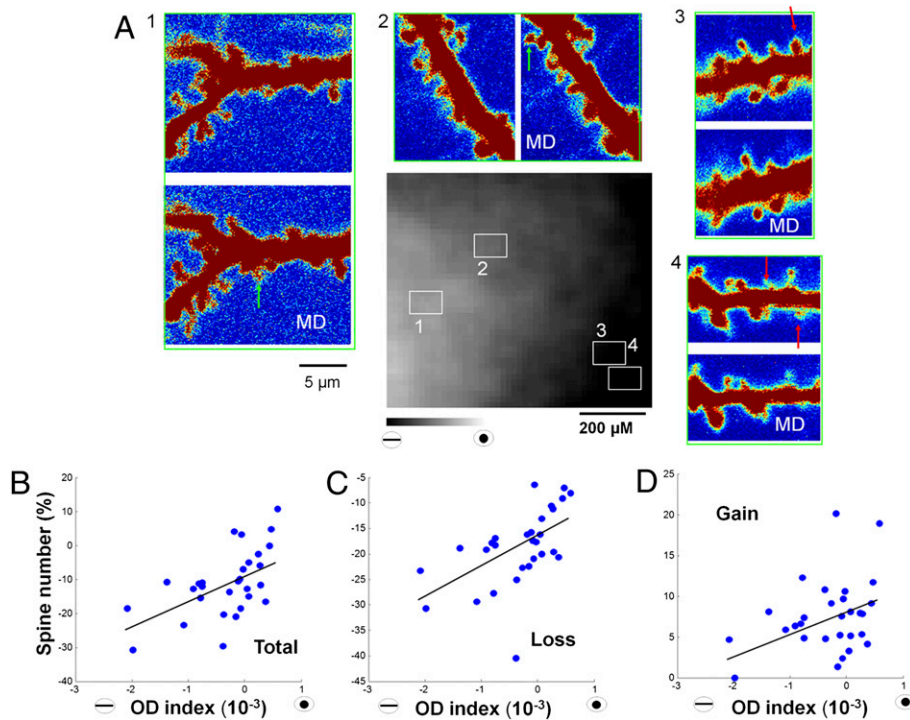


**Fig. 6.** Dendritic spine remodeling correlates with functional changes in defined OD regions within V1. (A) Spine turnover in four regions (marked 1–4 with squares in OD map, Center) with different OD preferences after 6 h of MD. Green arrows, new spines; red arrows, lost spines. (B–D) Rates of change of total number (B), loss (C), and gain (D) of spines as a function of ODI at each of 29 sites. Each site includes the analysis of all spines in an  $80 \times 60\text{-}\mu\text{m}$  region, and corresponds to a region of  $6 \times 4$  pixels in the intrinsic signal imaging map (SI Materials and Methods). ODI was less than  $-0.001$  at four sites with 436 spines; greater than  $-0.001$  and less than 0 at 15 sites with 1,155 spines, and between 0 and 0.001 at 10 sites with 1,015 spines.

remodels circuitry rapidly based on the amount of drive to individual neurons. It is interesting to note that, in one animal, we observed a clear enhancement of open eye drive after short-term MD, and we observed a tendency toward a gain in spines in nondeprived eye-dominated regions. Potentiation of the nondeprived eye is largely thought to be a slower process that relies on a previous reduction in the strength of the deprived eye and is mediated by different mechanisms (6, 7, 33). Future studies will need to examine whether there is a rapid change in nondeprived eye responses after short-term MD that occurs concurrently with deprived eye depression.

**Experience-Dependent Structural Remodeling of Visual Cortex Synapses.** In the visual cortex, dendritic spine structure and density are sensitive to visual stimulation (23, 34). In the mouse, MD and binocular deprivation destabilize spines during the critical period (25, 31), and MD in adults results in spine gain, which mirrors increases in nondeprived eye drive (35). Here we show that, during the critical period, changes in visual function are accompanied by a rapid spine loss in areas that experience a loss in deprived eye responses. Although previous changes in dendritic spine density have been described to be on the order of days in vivo (36–39), here we show that dendritic spine turnover can be very rapid, and significant spine loss and gain can be observed alongside altered functional responses in as little as a few hours after MD.

Although the correlation between spine motility or turnover and function has been explored in the mouse, this is, to our knowledge, the first study that attempts to explore this relationship in a more established model of visual function. The mouse visual cortex exhibits robust OD plasticity (3), but it lacks OD columns, which are prominent in ferrets, cats, and primates, precluding an analysis of structural changes in different OD domains. Pairing two different optical techniques in the ferret allowed us to assay structural and functional aspects of different cortical regions. Our work shows that structural and functional remodeling occur on similar timescales and are regulated by the same rules, occurring globally within the cortex, suggesting that remodeling of connectivity by alterations at the level of dendritic spines is an important

component of OD plasticity. A previous study in the cat found little change in synapse number following short-term MD (12). It is possible that dynamic imaging of the same dendritic sections before and after MD allowed us to detect subtle changes that are easily missed when comparing static images in a population of animals. It is important to note, however, that the ferret visual cortex, although a well studied model of visual plasticity, exhibits some distinct features as well, such as relatively large contralateral eye regions within the central visual field representation of V1. It will be interesting to compare our results with those obtained in cats or primates in the future.

Another important issue is that our analysis is predicated on the fact that the OD tuning of individual spines within our two-photon images follows our intrinsic signal OD map. Because it is likely that the inputs are more broadly tuned than the individual neuron on which they impinge, the correlation between the structural and functional changes we measure is likely to be imperfect. To ensure that this was a relatively small effect and that the majority of the imaged spines had properties that reflected the OD map, we carried out two-photon calcium imaging paired with intrinsic signal imaging (40) in young ferrets. We found that the tuning of the neuropil, which largely reflects input tuning, was very closely aligned with the intrinsic signal map (Fig. S8), suggesting that, in fact, the majority of the inputs were tuned similarly. Although these data support our approach, in the future, it would be interesting to probe the tuning of individual spines by using recently introduced calcium imaging approaches (41) to determine whether spines with distinct tuning properties behave differently following MD.

**Recovery from MD.** Although recovery from MD has been shown to rely in part on different mechanisms than the initial MD (8, 42), its progression is not well understood. Here we show that recovery from MD can be equally rapid and robust as the effects of initial MD and that even a few hours of eye opening can substantially reverse the effects of a week-long MD in ferrets. Additionally, as little as 24 h of eye opening can increase dendritic spine remodeling and return dendritic spine numbers to their pre-MD levels.

Although intracortical axonal remodeling in the visual cortex has not been examined, it is interesting to note that the short MD duration used here is unlikely to allow enough time for axonal remodeling, as evidenced by studies on geniculocortical afferents (43), suggesting that the presynaptic network remains intact until the deprived eye is reopened. This stable presynaptic scaffold could serve to allow fast recovery of binocularity by guiding the regrowth of synaptic protrusions at preexisting locations. Such a structural synaptic “trace” on the dendritic spine level was recently described in the adult visual cortex after MD (35). Dendritic spines formed during a first MD episode were not eliminated but shrunk following eye reopening and enlarged during a second MD episode, possibly allowing the faster implementation of plasticity during the second MD. In our experiments, approximately 40% of spines reappeared within 0.5  $\mu\text{m}$  of a location where a spine was lost during the MD period, suggesting that such a presynaptic trace may exist. The fact that the majority of spine gain did not occur preferentially at locations of lost spines suggests, however, that during recovery many spines are formed de novo with new presynaptic partners.

## Materials and Methods

Sixteen ferrets were used in these experiments. All experiments were performed under protocols approved by Animal Care and Use Committee of the Massachusetts Institute of Technology and conformed to National Institutes of Health guidelines.

**Animal Preparation.** A detailed description of animal preparation is provided in *SI Materials and Methods*. Anesthetized ferrets were given cortical injections

of EGFP-expressing Sindbis virus, and craniotomies were sealed and covered with a transparent window to allow for multiple imaging sessions.

**Optical Imaging.** The details of optical imaging have been described elsewhere (28), and are repeated in brief in *SI Materials and Methods*.

**Two-Photon Imaging.** A custom-made two-photon laser-scanning microscope based on a modified Fluoview confocal scanhead (Olympus) and a tunable Ti:S laser (Tsunami; Spectra-physics) was used for imaging. Images were collected by using Fluoview software and analyzed in Matlab. Acquisition and analysis are detailed further in *SI Materials and Methods*.

**ODI of Spines.** Blood vessel maps were obtained during intrinsic signal and two-photon imaging (*SI Materials and Methods*). Images were aligned by using these maps. The ODI of each spine site was determined by the averaged ODI across the corresponding pixels of the intrinsic signal image.

**Simulation of MD Effects.** Details of the models used to simulate MD effects are given in *SI Materials and Methods*.

**Statistical Analyses.** Standard *t* tests were used for all comparisons;  $P < 0.05$  was considered statistically significant. Data are presented as mean  $\pm$  SEM.

**ACKNOWLEDGMENTS.** We thank Travis Emery for assistance, and members of the M.S. laboratory for their help and advice. This work was funded by National Institutes of Health Grants EY007023 (to M.S.), EY017098 (to M.S.), and EY019277 (to A.K.M.); 973(2010CB327901), Doctoral Fund, Shanghai Pujiang, Shu Guang and Education Commission Programs from China (to H.Y.); the Burroughs-Wellcome Career Award in the biological sciences (to A.K.M.); an Arthur. P. Sloan Fellowship (to A.K.M.); and a grant from the Whitehall Foundation (to A.K.M.).

- Wiesel TN, Hubel DH (1963) Single-cell responses in striate cortex of kittens deprived of vision in one eye. *J Neurophysiol* 26:1003–1017.
- Hubel DH, Wiesel TN (1970) The period of susceptibility to the physiological effects of unilateral eye closure in kittens. *J Physiol* 206:419–436.
- Gordon JA, Stryker MP (1996) Experience-dependent plasticity of binocular responses in the primary visual cortex of the mouse. *J Neurosci* 16:3274–3286.
- Issa NP, Trachtenberg JT, Chapman B, Zahs KR, Stryker MP (1999) The critical period for ocular dominance plasticity in the Ferret's visual cortex. *J Neurosci* 19:6965–6978.
- Mioche L, Singer W (1989) Chronic recordings from single sites of kitten striate cortex during experience-dependent modifications of receptive-field properties. *J Neurophysiol* 62:185–197.
- Frenkel MY, Bear MF (2004) How monocular deprivation shifts ocular dominance in visual cortex of young mice. *Neuron* 44:917–923.
- Kaneko M, Stellwagen D, Malenka RC, Stryker MP (2008) Tumor necrosis factor- $\alpha$  mediates one component of competitive, experience-dependent plasticity in developing visual cortex. *Neuron* 58:673–680.
- Kaneko M, Hanover JL, England PM, Stryker MP (2008) TrkB kinase is required for recovery, but not loss, of cortical responses following monocular deprivation. *Nat Neurosci* 11:497–504.
- Mitchell DE, Sengpiel F (2009) Neural mechanisms of recovery following early visual deprivation. *Philos Trans R Soc Lond B Biol Sci* 364:383–398.
- Antonini A, Stryker MP (1993) Rapid remodeling of axonal arbors in the visual cortex. *Science* 260:1819–1821.
- Shatz CJ, Stryker MP (1978) Ocular dominance in layer IV of the cat's visual cortex and the effects of monocular deprivation. *J Physiol* 281:267–283.
- Silver MA, Stryker MP (2000) Distributions of synaptic vesicle proteins and GAD65 in deprived and nondeprived ocular dominance columns in layer IV of kitten primary visual cortex are unaffected by monocular deprivation. *J Comp Neurol* 422:652–664.
- Trachtenberg JT, Stryker MP (2001) Rapid anatomical plasticity of horizontal connections in the developing visual cortex. *J Neurosci* 21:3476–3482.
- Gray EG (1959) Electron microscopy of synaptic contacts on dendrite spines of the cerebral cortex. *Nature* 183:1592–1593.
- Yuste R, Majewska A, Holthoff K (2000) From form to function: calcium compartmentalization in dendritic spines. *Nat Neurosci* 3:653–659.
- Dunaevsky A, Tashiro A, Majewska A, Mason C, Yuste R (1999) Developmental regulation of spine motility in the mammalian central nervous system. *Proc Natl Acad Sci USA* 96:13438–13443.
- Fischer M, Kaech S, Knutti D, Matus A (1998) Rapid actin-based plasticity in dendritic spines. *Neuron* 20:847–854.
- Majewska A, Tashiro A, Yuste R (2000) Regulation of spine calcium dynamics by rapid spine motility. *J Neurosci* 20:8262–8268.
- Matsuzaki M, Honkura N, Ellis-Davies GC, Kasai H (2004) Structural basis of long-term potentiation in single dendritic spines. *Nature* 429:761–766.
- Zhou Q, Homma KJ, Poo MM (2004) Shrinkage of dendritic spines associated with long-term depression of hippocampal synapses. *Neuron* 44:749–757.
- Engert F, Bonhoeffer T (1999) Dendritic spine changes associated with hippocampal long-term synaptic plasticity. *Nature* 399:66–70.
- Tropea D, Majewska AK, Garcia R, Sur M (2010) Structural dynamics of synapses in vivo correlate with functional changes during experience-dependent plasticity in visual cortex. *J Neurosci* 30:11086–11095.
- Wallace W, Bear MF (2004) A morphological correlate of synaptic scaling in visual cortex. *J Neurosci* 24:6928–6938.
- Mataga N, Mizuguchi Y, Hensch TK (2004) Experience-dependent pruning of dendritic spines in visual cortex by tissue plasminogen activator. *Neuron* 44:1031–1041.
- Oray S, Majewska A, Sur M (2004) Dendritic spine dynamics are regulated by monocular deprivation and extracellular matrix degradation. *Neuron* 44:1021–1030.
- Jeromin A, Yuan LL, Frick A, Pfaffinger P, Johnston D (2003) A modified Sindbis vector for prolonged gene expression in neurons. *J Neurophysiol* 90:2741–2745.
- White LE, Bosking WH, Williams SM, Fitzpatrick D (1999) Maps of central visual space in ferret V1 and V2 lack matching inputs from the two eyes. *J Neurosci* 19:7089–7099.
- Yu H, Farley BJ, Jin DZ, Sur M (2005) The coordinated mapping of visual space and response features in visual cortex. *Neuron* 47:267–280.
- Harris KM, Kater SB (1994) Dendritic spines: Cellular specializations imparting both stability and flexibility to synaptic function. *Annu Rev Neurosci* 17:341–371.
- Rittenhouse CD, Majewska AK (2009) Synaptic mechanisms of activity-dependent remodeling in visual cortex. *J Exp Neurosci* 2:23–41.
- Majewska A, Sur M (2003) Motility of dendritic spines in visual cortex *in vivo*: Changes during the critical period and effects of visual deprivation. *Proc Natl Acad Sci USA* 100:16024–16029.
- Mower AF, et al. (2012) Experience-dependent regulation of CaMKII activity within single visual cortex synapses *in vivo*. *Proc Natl Acad Sci USA* 108:21246–21251.
- Mrsic-Flogel TD, et al. (2007) Homeostatic regulation of eye-specific responses in visual cortex during ocular dominance plasticity. *Neuron* 54:961–972.
- Valverde F (1967) Apical dendritic spines of the visual cortex and light deprivation in the mouse. *Exp Brain Res* 3:337–352.
- Hofer SB, Mrsic-Flogel TD, Bonhoeffer T, Hübener M (2009) Experience leaves a lasting structural trace in cortical circuits. *Nature* 457:313–317.
- Trachtenberg JT, et al. (2002) Long-term *in vivo* imaging of experience-dependent synaptic plasticity in adult cortex. *Nature* 420:788–794.
- Holtmaat A, Wilbrecht L, Knott GW, Welker E, Svoboda K (2006) Experience-dependent and cell-type-specific spine growth in the neocortex. *Nature* 441:979–983.
- Xu T, et al. (2009) Rapid formation and selective stabilization of synapses for enduring motor memories. *Nature* 462:915–919.
- Yang G, Pan F, Gan WB (2009) Stably maintained dendritic spines are associated with lifelong memories. *Nature* 462:920–924.
- Schummers J, Yu H, Sur M (2008) Tuned responses of astrocytes and their influence on hemodynamic signals in the visual cortex. *Science* 320:1638–1643.
- Chen X, Leischner U, Rochefort NL, Nelken I, Konnerth A (2011) Functional mapping of single spines in cortical neurons *in vivo*. *Nature* 475:501–505.
- Liao DS, Mower AF, Neve RL, Sato-Bigbee C, Ramoa AS (2002) Different mechanisms for loss and recovery of binocularity in the visual cortex. *J Neurosci* 22:9015–9023.
- Antonini A, Fagiolioli M, Stryker MP (1999) Anatomical correlates of functional plasticity in mouse visual cortex. *J Neurosci* 19:4388–4406.